

CHARACTERISTICS OF GUIDED MODES IN PLANAR CHIRAL NIHILITY META-MATERIAL WAVEGUIDES

J. Dong and C. Xu

Institute of Optical Fiber Communication and Network Technology
Ningbo University
Ningbo 315211, China

Abstract—The characteristics of guided modes in the planar waveguides which the core or cladding consists of chiral nihility meta-materials are studied theoretically. The dispersion curves, electromagnetic fields, energy flow distribution and the power of several low-order guided modes in the chiral nihility waveguides are presented. Some novel features such as anomalous dispersion curves, the power flows opposite to the wave vector propagation direction in the chiral nihility waveguides have been found.

1. INTRODUCTION

Studies on the propagation of electromagnetic waves in waveguides are important for device design. Recently, the negative refractive index materials (NIMs) have attracted much attention because NIM has many novel features and potential applications such as perfect lens. Various waveguides including NIM have been investigated intensively [1–11]. Many novel characteristics of guided waves in NIM waveguides were found. Guided modes in a slab of uniaxial backward-wave medium can carry energy in opposite directions inside and outside the slab with backward waves inside the slab [1]. Peculiar properties of guided waves in NIM slab waveguides include the absence of fundamental modes, mode double degeneracy, and the sign-varying energy flux [2]. Anomalous dispersion curves were revealed: Below cutoff, there is a frequency range for which there are two possible propagation coefficients [3]. There exists a sort of unique electromagnetic waves termed as “surface waves” whose electromagnetic fields exponentially decay on both sides of the

Corresponding author: J. Dong (dongjianfeng@nbu.edu.cn).

interfaces between NIM and conventional materials, and cannot exist in normal waveguides [4–6]. All surface plasmon polariton (so-called SPP) eigenmodes supported by generalized asymmetric slab heterostructures have been identified and classified [5]. Similar peculiar properties of guided modes and surface wave (SPP) are also found in the NIM grounded slab waveguides [7–9]. Waves in NIM waveguides can propagate very slowly and even can be stopped [10, 11].

On the other hand, waveguides including chiral media have been studied intensively because of their important potential applications in optics and microwaves [12–14]. More recently, the chiral medium has been suggested to achieve NIM [15–17]. It has been shown that the chirality parameter can be greater than refraction index at least near the resonant frequency, thus one eigen-wave in the chiral medium becomes a backward wave, making negative refraction in the chiral medium possible [16, 17]. The effective negative index of refraction in chiral meta-materials has been experimentally achieved at microwave frequencies [18] and THz frequencies [19] in 2009. The novel feature of guided modes in chiral negative refraction waveguides has been investigated theoretically [20–22]. Waves in the parallel-plate waveguide containing two-layer chiral nihility meta-materials (the chiral medium in which the permittivity and permeability are simultaneously zero) and one air layer [23], and in the grounded chiral nihility metamaterial slab has been examined [24].

In this paper, we firstly present the dispersion equations of general chiral planar waveguides in which both the core and cladding consist of chiral materials. Then two special cases: The planar waveguides consisting of a chiral nihility meta-material core with an achiral cladding and a chiral nihility meta-material cladding with an achiral core are examined in detail. For guided odd and even modes, the dispersion equations, normalized cutoff frequencies, electromagnetic fields, and energy flow of right-handed and left-handed circularly polarized (RCP and LCP) modes are derived in explicit forms. Numerical results of several low-order guided modes are given for typical chirality parameters. Some novel features such as anomalous dispersion curves and the power flows opposite to the wave vector propagation direction in the chiral nihility waveguides are found.

2. DISPERSION EQUATIONS OF GENERAL THREE-LAYERED PLANAR CHIRAL WAVEGUIDES

Consider three-layered symmetric planar chiral waveguides in which the core and cladding materials are chiral, as shown in Fig. 1. The thickness of the core is d . The constitutive relations in the chiral media

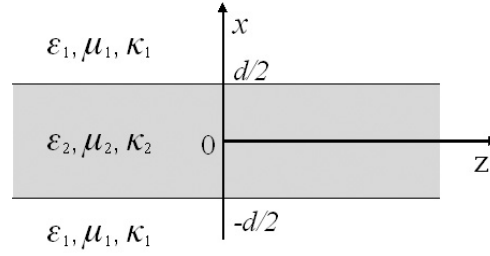


Figure 1. Geometry of the three-layered planar chiral waveguide.

adopted here for a time-harmonic field with $\exp(j\omega t)$ are as follows:

$$\mathbf{D} = \varepsilon_i \mathbf{E} - j\kappa_i \sqrt{\mu_0 \varepsilon_0} \mathbf{H}, \quad \mathbf{B} = \mu_i \mathbf{H} + j\kappa_i \sqrt{\mu_0 \varepsilon_0} \mathbf{E} \quad (1)$$

where $\mu_i, \varepsilon_i, \kappa_i$ ($i = 1, 2$) are permeability, permittivity and chirality parameter, respectively.

In the chiral medium, electromagnetic fields can be expressed as [17]:

$$\mathbf{E} = \mathbf{E}_+ + \mathbf{E}_-, \quad \mathbf{H} = \mathbf{H}_+ + \mathbf{H}_- \quad (2)$$

The relationship between electric and magnetic fields is

$$\mathbf{H}_\pm = \pm j \cdot \mathbf{E}_\pm / \eta_i \quad (3)$$

where \mathbf{E}_+ and \mathbf{E}_- are solutions of the wave equations:

$$(\nabla^2 + k_{i+}^2) \mathbf{E}_+ = 0, \quad (\nabla^2 + k_{i-}^2) \mathbf{E}_- = 0 \quad (4)$$

where $k_{i\pm} = n_{i\pm} k_0$, and $n_{i\pm} = n_i \pm \kappa_i$ are the effective refractive index of the two eigen-waves (the subscription + and - correspond to right- and left-handed circularly polarized waves, respectively denoted as RCP and LCP) in the chiral media; $k_0 = \omega \sqrt{\mu_0 \varepsilon_0}$, $n_i = \sqrt{\mu_i \varepsilon_i / \mu_0 \varepsilon_0}$ and $\eta_i = \sqrt{\mu_i / \varepsilon_i}$ are the wavenumber in free space, the refractive index and wave impedance of the chiral medium. If the chirality parameter is very large ($\kappa_i > n_i$), then the effective refractive index n_{i-} for the LCP eigen-wave is negative ($n_{i-} < 0$). We call this type of strong chiral medium as chiral negative refraction medium.

Because the planar chiral waveguide structure is symmetry to x -axis, we can express the solutions of the longitudinal-field component in Equation (4) as [14]:

$$E_{z\pm} = \begin{cases} A_\pm \sin(k_{x\pm} x) & |x| < d/2 \\ B_\pm \exp[-\gamma_{x\pm} (|x| - d/2)] & |x| > d/2 \end{cases} \quad (5)$$

for guided odd modes, and

$$E_{z\pm} = \begin{cases} A_{\pm} \cos(k_{x\pm}x) & |x| < d/2 \\ B_{\pm} \exp[-\gamma_{x\pm}(|x| - d/2)] & |x| > d/2 \end{cases} \quad (6)$$

for guided even modes, where $\exp[j(\omega t - \beta z)]$ is omitted for simplicity and β is the longitudinal propagation constant, the parameters $k_{x\pm}, \gamma_{x\pm}$ are $k_{x\pm} = (k_{2\pm}^2 - \beta^2)^{1/2}, \gamma_{x\pm} = (\beta^2 - k_{1\pm}^2)^{1/2}$.

The relationship between the transversal and longitudinal electromagnetic field components can be found in [12]. According to the boundary condition (continuity of the tangential fields) for electromagnetic field components at $x = d/2$, the dispersion equations of guided modes in the planar chiral waveguides can be derived as follows:

$$\begin{aligned} & \left(\frac{k_{1+}}{\gamma_{x+}} \sin u_+ - \frac{k_{2+}}{k_{x+}} \cos u_+ \right) \left(-\frac{k_{1-}}{\gamma_{x-}} \sin u_- + \frac{k_{2-}}{k_{x-}} \cos u_- \right) (\eta_1 + \eta_2)^2 \\ & + \left(\frac{k_{1-}}{\gamma_{x-}} \sin u_+ + \frac{k_{2+}}{k_{x+}} \cos u_+ \right) \left(\frac{k_{1+}}{\gamma_{x+}} \sin u_- + \frac{k_{2-}}{k_{x-}} \cos u_- \right) (\eta_1 - \eta_2)^2 = 0 \end{aligned} \quad (7)$$

for guided odd modes, and

$$\begin{aligned} & \left(\frac{k_{1+}}{\gamma_{x+}} \cos u_+ + \frac{k_{2+}}{k_{x+}} \sin u_+ \right) \left(\frac{k_{1-}}{\gamma_{x-}} \cos u_- + \frac{k_{2-}}{k_{x-}} \sin u_- \right) (\eta_1 + \eta_2)^2 \\ & + \left(\frac{k_{1-}}{\gamma_{x-}} \cos u_+ - \frac{k_{2+}}{k_{x+}} \sin u_+ \right) \left(-\frac{k_{1+}}{\gamma_{x+}} \cos u_- + \frac{k_{2-}}{k_{x-}} \sin u_- \right) (\eta_1 - \eta_2)^2 = 0 \end{aligned} \quad (8)$$

for guided even modes, where $u_{\pm} = k_{x\pm}d/2$. These dispersion equations are consistent with those in [14]. However, the constitutive relations adopted here are different, and there were many typo mistakes in dispersion relation formula in [14].

In the next sections, we will focus on the two special cases: The planar waveguides consisting of a chiral nihility core with an achiral cladding and a chiral nihility cladding with an achiral core. The chiral nihility means $\mu_i = 0, \varepsilon_i = 0, \kappa_i \neq 0$.

3. GUIDED MODES IN PLANAR CHIRAL NIHILITY CORE WAVEGUIDES

When the core is a chiral nihility meta-material and cladding is an achiral medium, the above parameters become $k_{2\pm} = \pm\kappa_2 k_0, k_{x\pm} = (k_{2\pm}^2 - \beta^2)^{1/2} = (\kappa_2^2 k_0^2 - \beta^2)^{1/2} = k_x, \gamma_{x\pm} = (\beta^2 - k_{1\pm}^2)^{1/2} = (\beta^2 - k_1^2)^{1/2} = \gamma_x, u_{\pm} = k_{x\pm}d/2 = k_x d/2 = u$. It is shown that both the dispersion Equations (7) and (8) can be divided into two equations which correspond to RCP and LCP modes, respectively. For guided odd and even modes, the dispersion equations, normalized cutoff frequencies, electromagnetic fields, and energy flow of RCP and LCP modes are obtained as follows.

3.1. Odd Modes

3.1.1. Dispersion Equation

The dispersion equations are:

$$(\kappa_2^2 k_0^2 - \beta^2)^{1/2} \frac{d}{2} = \tan^{-1} \left[\frac{\kappa_2 k_0}{k_1} \left(\frac{\beta^2 - k_1^2}{\kappa_2^2 k_0^2 - \beta^2} \right)^{1/2} \right] + m\pi, \quad m=0, 1, 2, \dots \quad (9)$$

for RCP odd modes, and

$$(\kappa_2^2 k_0^2 - \beta^2)^{1/2} \frac{d}{2} = -\tan^{-1} \left[\frac{\kappa_2 k_0}{k_1} \left(\frac{\beta^2 - k_1^2}{\kappa_2^2 k_0^2 - \beta^2} \right)^{1/2} \right] + m\pi, \quad m=1, 2, 3, \dots \quad (10)$$

for LCP odd modes, where m is mode number. It is noted that m starts from 0 for RCP odd modes and from 1 for LCP odd modes.

3.1.2. Normalized Cutoff Frequency

The normalized cutoff frequencies can be obtained from the dispersion Equations (9) and (10) by setting $\beta \rightarrow k_1$:

$$(k_0 d)_c = \frac{2m\pi}{(\kappa_2^2 - n_1^2)^{1/2}}, \quad m=0, 1, 2, \dots \quad (11)$$

for RCP odd modes, and

$$(k_0 d)_c = \frac{2m\pi}{(\kappa_2^2 - n_1^2)^{1/2}}, \quad m=1, 2, 3, \dots \quad (12)$$

for LCP odd modes.

3.1.3. Electromagnetic Field

The electromagnetic fields can be derived directly in explicit forms; here only $x > 0$ region are presented; and $x < 0$ region can be obtained according to symmetry.

In the core $x < d/2$, the electric fields for both RCP and LCP odd modes are:

$$\begin{cases} E_x = -\frac{j\beta}{k_x} \frac{C}{\sin(u)} \cos(k_x x) \\ E_y = -\frac{\kappa_2 k_0}{k_x} \frac{C}{\sin(u)} \cos(k_x x) \\ E_z = \frac{C}{\sin(u)} \sin(k_x x) \end{cases} \quad (13)$$

In the cladding $x > d/2$, the electric fields are:

$$\begin{cases} E_x = -\frac{j\beta}{\gamma_x} C e^{-\gamma_x(x-d/2)} \\ E_y = \mp \frac{k_1}{\gamma_x} C e^{-\gamma_x(x-d/2)} \\ E_z = C e^{-\gamma_x(x-d/2)} \end{cases} \quad (14)$$

for RCP (upper sign) and LCP (lower sign) odd modes, respectively where C is an arbitrary constant, which can be determined by total power.

The magnetic fields in the core and cladding are:

$$\begin{Bmatrix} H_x \\ H_y \\ H_z \end{Bmatrix} = \pm \frac{j}{\eta_1} \begin{Bmatrix} E_x \\ E_y \\ E_z \end{Bmatrix} \quad (15)$$

for RCP (upper sign) and LCP (lower sign) odd modes, respectively.

3.1.4. Energy Flow

Energy flow along the z -axis in the waveguides is defined by

$$S_z = \frac{1}{2} \text{Re}(\mathbf{E} \times \mathbf{H}^*) \cdot \hat{\mathbf{z}} = \frac{1}{2} \text{Re}(E_x H_y^* - E_y H_x^*) \quad (16)$$

In the core $x < d/2$, energy flow is:

$$S_z = \pm \frac{\beta \kappa_2 k_0}{\eta_1 k_x^2} \left| \frac{C}{\sin(u)} \right|^2 \cos^2(k_x x) \quad (17)$$

for RCP (upper sign) and LCP (lower sign) odd modes, respectively.

In the cladding $x > d/2$, energy flow is:

$$S_z = \frac{\beta k_1}{\eta_1 \gamma_x^2} |C|^2 e^{-2\gamma_x(x-d/2)} \quad (18)$$

for both RCP and LCP odd modes.

It is obvious from formulas (17), (18) that S_z is positive for RCP odd modes and negative for LCP odd modes in the core, and positive for both RCP and LCP odd modes in the cladding. It indicates that energy flow of LCP modes is in opposite directions in the core and cladding.

3.2. Even Mode

3.2.1. Dispersion Equation

The dispersion equations are:

$$(\kappa_2^2 k_0^2 - \beta^2)^{1/2} \frac{d}{2} = -\tan^{-1} \left[\frac{k_1}{\kappa_2 k_0} \left(\frac{\kappa_2^2 k_0^2 - \beta^2}{\beta^2 - k_1^2} \right)^{1/2} \right] + m\pi, \quad m = 1, 2, 3 \dots \quad (19)$$

for RCP even modes, and

$$(\kappa_2^2 k_0^2 - \beta^2)^{1/2} \frac{d}{2} = \tan^{-1} \left[\frac{k_1}{\kappa_2 k_0} \left(\frac{\kappa_2^2 k_0^2 - \beta^2}{\beta^2 - k_1^2} \right)^{1/2} \right] + m\pi, \quad m = 0, 1, 2 \dots \quad (20)$$

for LCP even modes.

It is noted that, in contrast to odd modes, m starts from 1 for RCP even modes and starts from 0 for LCP even modes.

3.2.2. Normalized Cutoff Frequency

The normalized cutoff frequencies can be obtained from the dispersion Equations (19) and (20) by setting $\beta \rightarrow k_1$:

$$(k_0 d)_c = \frac{(2m - 1)\pi}{(\kappa_2^2 - n_1^2)^{1/2}}, \quad m = 1, 2, 3 \dots \quad (21)$$

for RCP even modes, and

$$(k_0 d)_c = \frac{(2m + 1)\pi}{(\kappa_2^2 - n_1^2)^{1/2}}, \quad m = 0, 1, 2 \dots \quad (22)$$

for LCP even modes.

3.2.3. Electromagnetic Field

In the core $x < d/2$, the electric fields for both RCP and LCP even modes are:

$$\begin{cases} E_x = \frac{j\beta}{k_x} \frac{C}{\cos(u)} \sin(k_x x), \\ E_y = \frac{\kappa_2 k_0}{k_x} \frac{C}{\cos(u)} \sin(k_x x), \\ E_z = \frac{C}{\cos(u)} \cos(k_x x) \end{cases} \quad (23)$$

In the cladding $x > d/2$, the electric fields are the same as those for RCP and LCP odd modes (see Equation (14)).

The relationship between magnetic and electric fields in the core and cladding is also the same as that for RCP and LCP odd modes (see Equation (15)).

3.2.4. Energy Flow

In the core $x < d/2$, energy flow is:

$$S_z = \pm \frac{\beta \kappa_2 k_0}{\eta_1 k_x^2} \left| \frac{C}{\cos(u)} \right|^2 \sin^2(k_x x) \quad (24)$$

for RCP (upper sign) and LCP (lower sign) odd modes, respectively.

In the cladding $x > d/2$, the formulas of energy flow are the same as those for RCP and LCP odd modes (see Equation (18)).

3.3. Numerical Example

The propagation constants can be calculated numerically from the dispersion equations (9), (10), (19), (20), then the electromagnetic fields and the energy flow distribution can be obtained. The normalized total power can be expressed as [2]

$$P = \frac{P_1 + P_2}{|P_1| + |P_2|} \quad (25)$$

where $P_1 = 2 \int_{d/2}^{\infty} S_z dx$ and $P_2 = \int_{-d/2}^{d/2} S_z dx$ are the power in the cladding and core, respectively. In this section, we present typical numerical results for the parameters in the core and cladding being $\mu_2 = \varepsilon_2 = 0$, $\kappa_2 = 1.5$ and $\mu_1 = \mu_0$, $\varepsilon_1 = \varepsilon_0$, $\kappa_1 = 0$.

Figure 2 shows the dispersion curves of several low-order guided odd and even modes in the planar chiral nihility core waveguide, where $n_{eff} = \beta/k_0$ is the effective refractive index; $k_0 d$ is the normalized frequency. Dashed and solid curves correspond to the odd and even modes, respectively. For RCP odd and even modes, the curves of effective refractive index versus normalized frequency increases monotonically, and the normalized cutoff frequencies (points C_1, C_2 , when $n_{eff} = 1$) satisfy Equation (11) or (21). However, for LCP odd and even modes, dispersion curves are no longer increasing monotonically, but are bent, and the cutoff frequencies (when $n_{eff} = 1$) are not the minimum frequencies that waves can propagate. When $m = 0$, there is one solution below cutoff frequency (point C_1) for LCP even mode in some frequency region. When $m = 1$, there are two solutions below cutoff frequencies (points C_2, C_3) for both LCP even and odd modes in some frequency region. Thus the cutoff frequencies

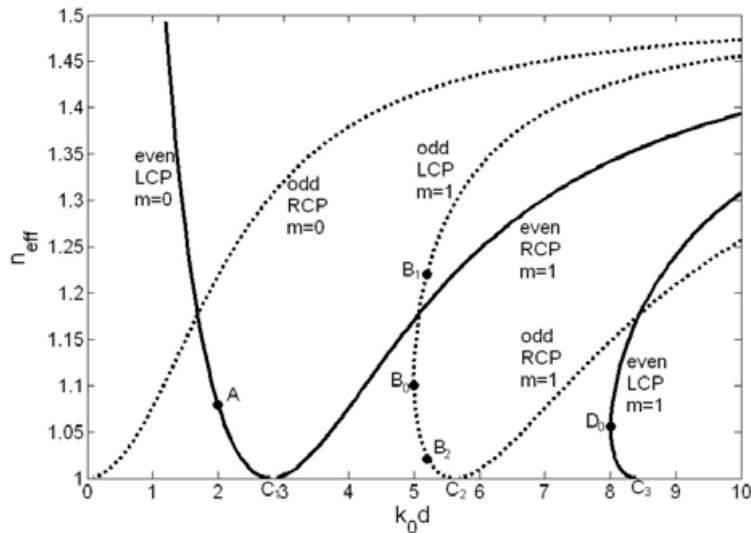


Figure 2. Dispersion curves of guided modes in the planar chiral nihility core waveguide.

here are not really “cutoff”. The real “cutoff” frequencies correspond to the minimum frequencies (critical points B_0, D_0) that guided wave can propagate. As the normalized frequency increases from the critical points B_0, D_0 , dispersion curves bifurcate two branches, which the effective refractive index increases for upper branch and decreases to $n_{eff} = 1$ for lower branch.

Figures 3 and 4 show the amplitudes of electromagnetic field components and energy flux distribution at normalized frequency $k_0 d = 2$ (point A in Fig. 2) for LCP even mode when $m = 0$. E_z, H_z are even functions of x (cos form) and E_x, E_y, H_x, H_y (sin form) are odd functions of x . S_z is negative in the core and positive in the cladding; the absolute power $|P_2|$ in the core is smaller than power P_1 in the cladding, thus the total power is positive.

Figures 5 and 6 show the amplitude of electromagnetic field components and energy flux distribution at normalized frequency $k_0 d = 5.2$ for LCP odd mode when $m = 1$. E_z, H_z are odd functions of x (sin form) and E_x, E_y, H_x, H_y (cos form) are even functions of x . S_z is negative in the core and positive in the cladding, too. However, there are two propagation constants at $k_0 d = 5.2$. For larger effective refractive index (point B_1 in upper branch dispersion curve in Fig. 2) $n_{eff} = 1.2224$, the absolute power $|P_2|$ is larger in the core than power

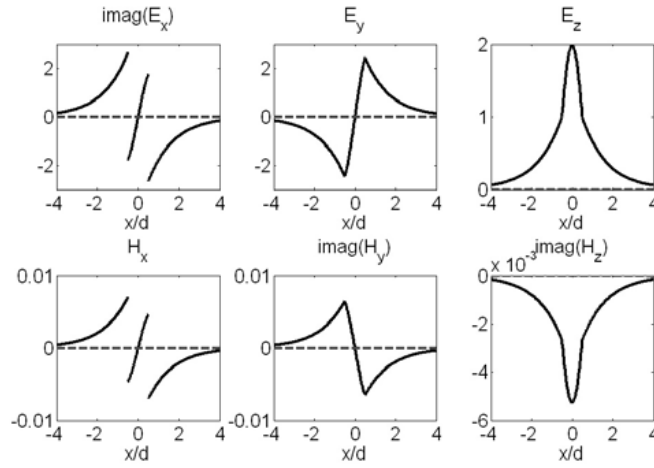


Figure 3. Amplitudes of electromagnetic field components at $k_0d = 2$ for LCP even mode when $m = 0$.

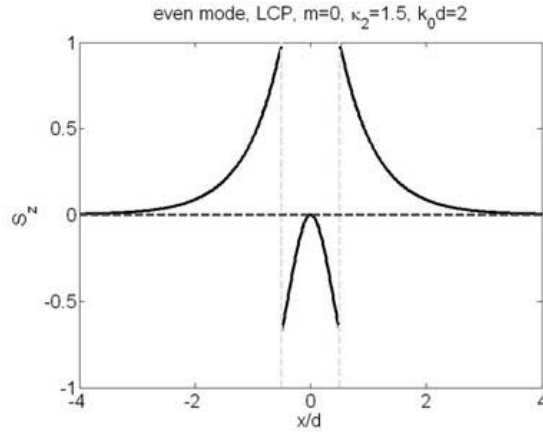


Figure 4. Energy flux at $k_0d = 2$ for LCP even mode when $m = 0$.

P_1 in the cladding, thus the total power is negative. For smaller effective refractive index (point B_2 in lower branch dispersion curve in Fig. 2), $n_{eff} = 1.0237$, the absolute power $|P_2|$ is smaller in the core than power P_1 in the cladding, thus the total power is positive.

The normalized total power P versus normalized frequency k_0d is plotted in Fig. 7 for three LCP modes (bended dispersion curves). For LCP even mode when $m = 0$, P decreases as k_0d decreases; however, it is always positive. It indicates that the absolute power in the core

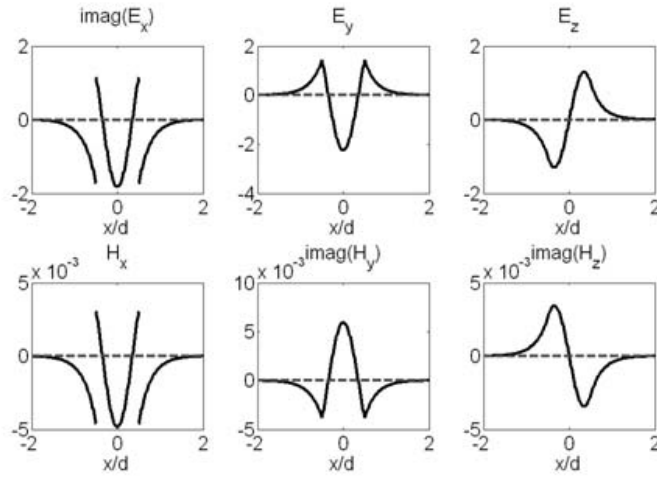


Figure 5. Amplitude of electromagnetic components at $k_0d = 5.2$ for LCP odd mode when $m = 1, n_{eff} = 1.2224$.

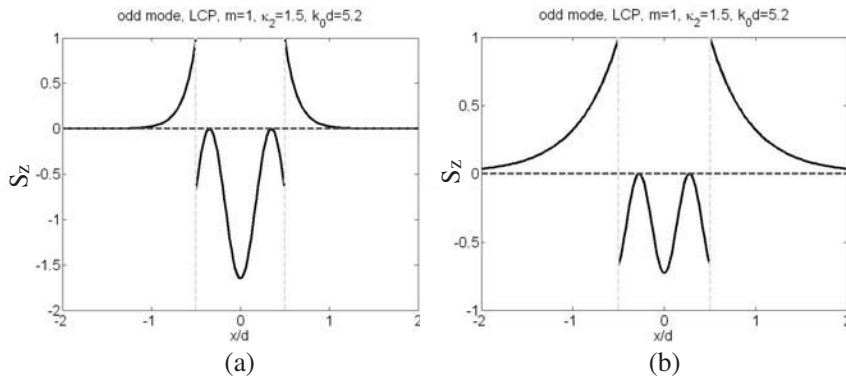


Figure 6. Energy flux at $k_0d = 5.2$ for LCP odd mode when $m = 1$, (a) $n_{eff} = 1.2224$; (b) $n_{eff} = 1.0237$.

is always smaller than that in the cladding. For LCP odd mode when $m = 1$, P is negative for upper branch dispersion curve and positive for lower branch dispersion curve. For upper branch dispersion curve, amplitude of P decreases from nearly -1 to 0 as k_0d decreases from 10 to 5 (critical point B_0 in Fig. 2). It implies that at critical point, the waveguide cannot propagate energy. For lower branch dispersion curve, P increases as k_0d increases from critical point B_0 to cutoff frequency C_2 . The similar results is observed for LCP even mode when

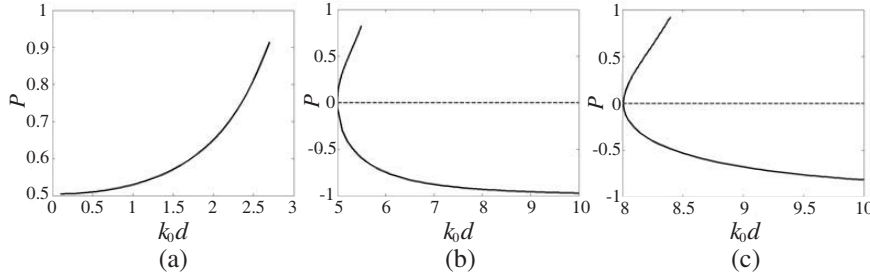


Figure 7. Normalized total power versus normalized frequency for (a) LCP even mode, $m = 0$; (b) LCP odd mode, $m = 1$; (c) LCP even mode, $m = 1$.

$m = 1$. It is noted that for RCP odd and even modes, the power both in the core and in the cladding are positive and the total power always positive. The reason of above results is that LCP is backward (negative refraction) wave and RCP is forward (positive refraction) wave in the chiral nihility meta-material, which means energy flow along the z -axis is negative for LCP waves and positive for RCP waves.

4. GUIDED MODES IN PLANAR CHIRAL NIHILITY CLADDING WAVEGUIDES

When the cladding is a chiral nihility meta-material and core is an achiral medium, the above parameters become $k_{x\pm} = (k_{2\pm}^2 - \beta^2)^{1/2} = (k_2^2 - \beta^2)^{1/2} = k_x$, $k_{1\pm} = \pm\kappa_1 k_0$, $\gamma_{x\pm} = (\beta^2 - k_{1\pm}^2)^{1/2} = (\beta^2 - \kappa_1^2 k_0^2)^{1/2} = \gamma_x$, $u_{\pm} = k_{x\pm} d/2 = k_x d/2 = u$. It is also shown that both the dispersion Equations (7) and (8) can be divided into two equations which correspond to RCP and LCP modes, respectively. For guided odd and even modes, the dispersion equations, normalized cutoff frequencies, electromagnetic fields, and energy flow of RCP and LCP modes are also obtained as follows.

4.1. Odd Mode

4.1.1. Dispersion Equation

The dispersion equation is

$$(k_2^2 - \beta^2)^{1/2} \frac{d}{2} = \tan^{-1} \left[\frac{k_2}{\kappa_1 k_0} \left(\frac{\beta^2 - \kappa_1^2 k_0^2}{k_2^2 - \beta^2} \right)^{1/2} \right] + m\pi, \quad m = 0, 1, 2, \dots \quad (26)$$

for RCP odd modes, and

$$(k_2^2 - \beta^2)^{1/2} \frac{d}{2} = -\tan^{-1} \left[\frac{k_2}{\kappa_1 k_0} \left(\frac{\beta^2 - \kappa_1^2 k_0^2}{k_2^2 - \beta^2} \right)^{1/2} \right] + m\pi, \quad m = 1, 2, 3 \dots \quad (27)$$

for LCP odd modes, where m is mode number.

4.1.2. Normalized Cutoff Frequency

The normalized cutoff frequencies can be obtained from the dispersion Equations (26) and (27) by setting $\beta \rightarrow \kappa_1 k_0$:

$$(k_0 d)_c = \frac{2m\pi}{(n_2^2 - \kappa_1^2)^{1/2}}, \quad m = 0, 1, 2 \dots \quad (28)$$

for RCP odd modes, and

$$(k_0 d)_c = \frac{2m\pi}{(n_2^2 - \kappa_1^2)^{1/2}}, \quad m = 1, 2, 3 \dots \quad (29)$$

for LCP odd modes.

4.1.3. Electromagnetic Field

In the core $x < d/2$, the electric fields are:

$$\begin{cases} E_x = -\frac{j\beta}{k_x} A \cos(k_x x) \\ E_y = \mp \frac{k_2}{k_x} A \cos(k_x x) \\ E_z = A \sin(k_x x) \end{cases} \quad (30)$$

for RCP (upper sign) and LCP (lower sign) odd modes, respectively.

In the cladding $x > d/2$, the electric fields for both RCP and LCP odd modes are:

$$\begin{cases} E_x = -\frac{j\beta}{\gamma_x} A \sin(u) e^{-\gamma_x(x-d/2)} \\ E_y = -\frac{\kappa_1 k_0}{\gamma_x} A \sin(u) e^{-\gamma_x(x-d/2)} \\ E_z = A \sin(u) e^{-\gamma_x(x-d/2)} \end{cases} \quad (31)$$

where A is a arbitrary constant.

The magnetic fields in the core and cladding are:

$$\begin{Bmatrix} H_x \\ H_y \\ H_z \end{Bmatrix} = \pm \frac{j}{\eta_2} \begin{Bmatrix} E_x \\ E_y \\ E_z \end{Bmatrix} \quad (32)$$

for RCP (upper sign) and LCP (lower sign) odd modes, respectively.

4.1.4. Energy Flow

In the core $x < d/2$, energy flow is:

$$S_z = \frac{\beta k_2}{\eta_2 k_x^2} |A|^2 \cos^2(k_x x) \quad (33)$$

for both RCP and LCP odd modes.

In the cladding $x > d/2$, energy flow is:

$$S_z = \pm \frac{\beta \kappa_1 k_0}{\eta_2 \gamma_x^2} |A|^2 \sin^2(u) e^{-2\gamma_x(x-d/2)} \quad (34)$$

for RCP (upper sign) and LCP (lower sign) odd modes, respectively.

It is obvious from formulas (33), (34) that S_z is positive for both RCP and LCP modes in the core, and positive for RCP odd modes and negative for LCP odd modes in the cladding. It also indicates that energy flow of LCP modes is in opposite directions in the core and cladding.

4.2. Even Mode

4.2.1. Dispersion Equation

The dispersion equations are:

$$(k_2^2 - \beta^2)^{1/2} \frac{d}{2} = -\tan^{-1} \left[\frac{\kappa_1 k_0}{k_2} \left(\frac{k_2^2 - \beta^2}{\beta^2 - \kappa_1^2 k_0^2} \right)^{1/2} \right] + m\pi, \quad m = 1, 2, 3 \dots \quad (35)$$

for RCP even modes, and

$$(k_2^2 - \beta^2)^{1/2} \frac{d}{2} = \tan^{-1} \left[\frac{\kappa_1 k_0}{k_2} \left(\frac{k_2^2 - \beta^2}{\beta^2 - \kappa_1^2 k_0^2} \right)^{1/2} \right] + m\pi, \quad m = 0, 1, 2 \dots \quad (36)$$

for LCP even modes.

4.2.2. Normalized Cutoff Frequency

The normalized cutoff frequencies can be obtained from the dispersion Equations (35) and (36) by setting $\beta \rightarrow \kappa_1 k_0$:

$$(k_0 d)_c = \frac{(2m-1)\pi}{(n_2^2 - \kappa_1^2)^{1/2}}, \quad m = 1, 2, 3 \dots \quad (37)$$

for RCP even modes, and

$$(k_0 d)_c = \frac{(2m+1)\pi}{(n_2^2 - \kappa_1^2)^{1/2}}, \quad m = 0, 1, 2 \dots \quad (38)$$

for LCP even modes.

4.2.3. Electromagnetic Field

In the core $x < d/2$, the electric fields are:

$$\begin{cases} E_x = \frac{j\beta}{k_x} A \sin(k_x x) \\ E_y = \pm \frac{k_2}{k_x} A \sin(k_x x) \\ E_z = A \cos(k_x x) \end{cases} \quad (39)$$

for RCP (upper sign) and LCP (lower sign) even modes, respectively.

In the cladding $x > d/2$, the electric fields for both RCP and LCP even modes are:

$$\begin{cases} E_x = -\frac{j\beta}{\gamma_x} A \cos(u) e^{-\gamma_x(x-d/2)} \\ E_y = -\frac{\kappa_1 k_0}{\gamma_x} A \cos(u) e^{-\gamma_x(x-d/2)} \\ E_z = A \cos(u) e^{-\gamma_x(x-d/2)} \end{cases} \quad (40)$$

The relationship between magnetic and electric fields in the core and cladding are also the same as those for RCP and LCP odd modes (see Equation (32)).

4.2.4. Energy Flow

In the core $x < d/2$, energy flow is:

$$S_z = \frac{\beta k_2}{\eta_2 k_x^2} |A|^2 \sin^2(k_x x) \quad (41)$$

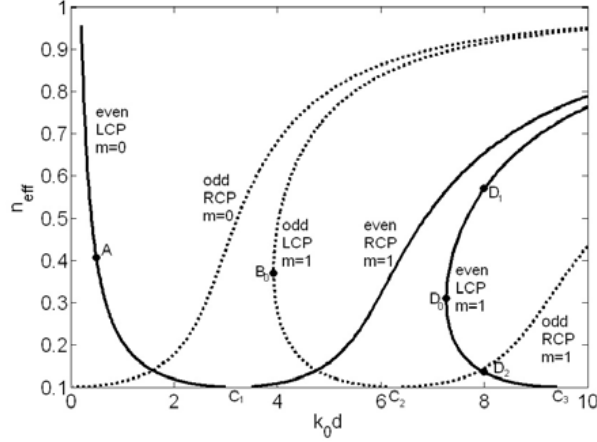


Figure 8. Dispersion curves of guided modes in the planar chiral nihility cladding waveguide.

for both RCP and LCP even modes.

In the cladding $x > d/2$, energy flow is:

$$S_z = \pm \frac{\beta \kappa_1 k_0}{\eta_2 \gamma_x^2} |A|^2 \cos^2(u) e^{-2\gamma_x(x-d/2)} \quad (42)$$

for RCP (upper sign) and LCP (lower sign) even modes, respectively.

4.3. Numerical Example

In this section, we present typical numerical results for the parameters in the core and cladding being $\mu_2 = \mu_0$, $\varepsilon_2 = \varepsilon_0$, $\kappa_2 = 0$ and $\mu_1 = \varepsilon_1 = 0$, $\kappa_1 = 0.1$. In contrast to Section 3.3, here the chirality parameter is smaller. This is an air-layer-open waveguide with chiral nihility meta-material cladding and is different from the structure in reference [23].

Figure 8 displays the dispersion curves of several low-order guided odd and even modes in the planar chiral nihility cladding waveguide. Dashed and solid curves correspond to the odd and even modes, respectively. The characteristics of dispersion curves are also anomalous and similar as Fig. 2 in Section 3.3.

The energy flux distribution at normalized frequency $k_0 d = 0.5$ (point A in dispersion curves in Fig. 8) for LCP even mode when $m = 0$ is shown in Fig. 9. S_z is positive in the core and negative in the cladding; the power P_2 in the core is much smaller than absolute power $|P_1|$ in the cladding, thus the total power is negative.

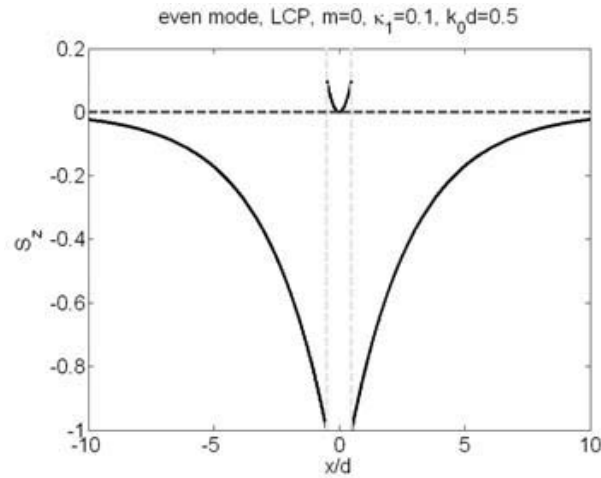


Figure 9. Energy flux at $k_0d = 0.5$ for LCP even mode when $m = 0$.

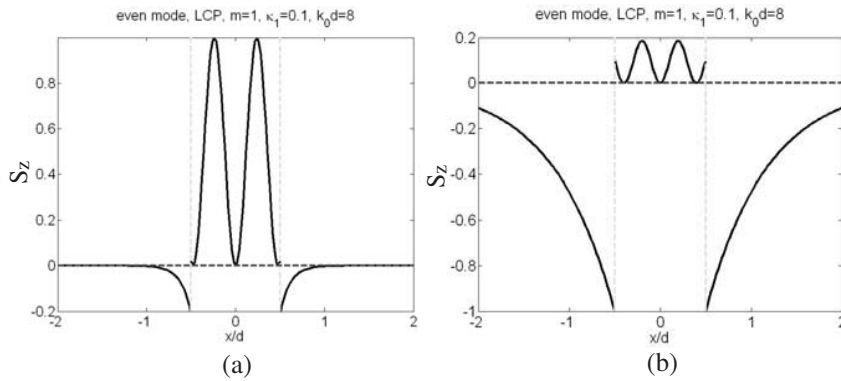


Figure 10. Energy flux at $k_0d = 8$ for LCP even mode when $m = 1$, (a) $n_{eff} = 0.5698$; (b) $n_{eff} = 0.1360$.

Figure 10 shows the energy flux distribution at normalized frequency $k_0d = 8$ for LCP even mode when $m = 1$. S_z is positive in the core and negative in the cladding, too. For larger effective refractive index (point D_1 in upper branch dispersion curve in Fig. 8) $n_{eff} = 0.5698$, the power P_2 is larger in the core than absolute power $|P_1|$ in the cladding, thus the total power is positive. For smaller effective refractive index (point D_2 in lower branch dispersion curve in Fig. 8), $n_{eff} = 0.1360$, the power P_2 is smaller in the core than absolute power $|P_1|$ in the cladding, thus the total power is negative.

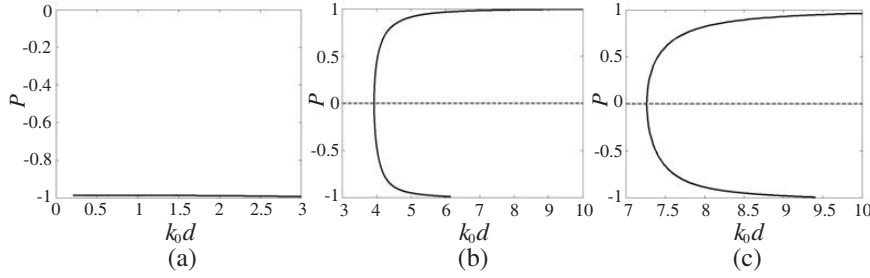


Figure 11. Total power versus normalized frequency for (a) LCP even mode, $m = 0$; (b) LCP odd mode, $m = 1$; (c) LCP even mode, $m = 1$.

The normalized total power P versus normalized frequency k_0d is plotted in Fig. 11 for three LCP modes (bended dispersion curves). For LCP even mode when $m = 0$, P is always near -1 as k_0d decreases. It indicates that the power P_2 in the core is much smaller than absolute power $|P_1|$ in the cladding. For LCP odd and even modes when $m = 1$, the results is similar to those in Section 3.3; however, the positive and negative are reversed.

5. CONCLUSION

The dispersion equations of general chiral planar waveguides in which both the core and cladding are chiral materials are presented. Guided modes in two special cases: Planar chiral nihility core or cladding waveguides are examined in detail. It has been shown that for guided odd and even modes in the chiral nihility waveguides, both the dispersion equations can be divided into two equations which correspond to RCP and LCP modes, respectively. For guided odd and even modes, the dispersion equations, normalized cutoff frequencies, electromagnetic fields, and energy flow of RCP and LCP modes are derived in explicit forms. Numerical results of several low-order guided modes are given for typical chirality parameters. Some novel features such as anomalous dispersion curves and the power flows opposite to the wave vector propagation direction in the chiral nihility waveguides have been found.

ACKNOWLEDGMENT

This work is supported by the National Basic Research Program (973) of China (2004CB719805), National Natural Science Foundation of

China (Grant No. 60777037) and is partially sponsored by K.C.Wong Magna Fund in Ningbo University.

REFERENCES

1. Lindell, I. V. and S. Ilvonen, "Waves in a slab of uniaxial BW medium," *Journal of Electromagnetic Waves and Applications*, Vol. 16, No. 3, 303–318, 2002.
2. Shadrivov, I. V., A. A. Sukhorukov, and Y. S. Kivshar, "Guided modes in negative-refractive-index waveguides," *Phys. Rev. E*, Vol. 67, 057602, 2003.
3. Cory, H. and A. Barger, "Surface-wave propagation along a metamaterial slab," *Microwave Opt. Technol. Lett.*, Vol. 38, No. 5, 392–395, 2003.
4. Wu, B.-I., T. M. Grzegorzczuk, Y. Zhang, and J. A. Kong, "Guided modes with imaginary transverse wave number in a slab waveguide with negative permittivity and permeability," *J. Appl. Phys.*, Vol. 93, No. 11, 9386–9388, 2003.
5. Tsakmakidis, K. L., C. Hermann, A. Klaedtke, C. Jamois, and O. Hess, "Surface plasmon polaritons in generalized slab heterostructures with negative permittivity and permeability," *Phys. Rev. B*, Vol. 73, 085104, 2006.
6. Wang, Z.-J. and J. Dong, "Analysis of guided modes in asymmetric left-handed slab waveguides," *Progress In Electromagnetics Research*, PIER 62, 203–215, 2006.
7. Mahmoud, S. F. and A. J. Viitanen, "Surface wave character on a slab of metamaterial with negative permittivity and permeability," *Progress In Electromagnetics Research*, PIER 51, 127–137, 2005.
8. Li, C., Q. Sui, and F. Li, "Complex guided wave solution of grounded dielectric slab made of metamaterials," *Progress In Electromagnetics Research*, PIER 51, 187–195, 2005.
9. Shu, W. and J.-M. Song, "Complete mode spectrum of a grounded dielectric slab with double negative metamaterials," *Progress In Electromagnetics Research*, PIER 65, 103–123, 2006.
10. Tsakmakidis, K. L., A. D. Boardman, and O. Hess, "Trapped rainbow' storage of light in metamaterials," *Nature*, Vol. 450, 397–401, 2007.
11. Jiang, T., J. Zhao, and Y. Feng, "Stopping light by an air waveguide with anisotropic metamaterial cladding," *Opt. Express*, Vol. 17, 170–177, 2009.
12. Oksanen, M., P. K. Koivisto, and I. V. Lindell, "Dispersion curves

- and fields for a chiral slab waveguide,” *IEE Proc. H Microwave Ant. Prop.*, Vol. 138, 327–334, 1991.
13. Mariotte, F., P. Pelet, and N. Engheta, “A review of recent study of guided waves in chiral media,” *Progress In Electromagnetics Research*, PIER 09, 311–350, 1994.
 14. Flood, K. M. and D. L. Jaggard, “Single-mode operation in symmetric planar waveguides using isotropic chiral media,” *Opt. Lett.*, Vol. 21, No. 7, 474–476, 1996.
 15. Tretyakov, S., I. Nefedov, A. Sihvola, S. Maslovski, and C. Simovski, “Waves and energy in chiral nihility,” *Journal of Electromagnetic Waves and Applications*, Vol. 17, 695–706, 2003.
 16. Pendry, J. B., “A chiral route to negative refraction,” *Science*, Vol. 306, 1353–1355, 2004.
 17. Tretyakov, S., A. Sihvola, and L. Jylhä, “Backward-wave regime and negative refraction in chiral composites,” *Photonics and Nanostructures*, Vol. 3, 107–115, 2005.
 18. Plum, E., J. Zhou, J. Dong, V. A. Fedotov, T. Koschny, C. M. Soukoulis, and N. I. Zheludev, “Metamaterial with negative index due to chirality,” *Phys. Rev. B*, Vol. 79, 035407, 2009.
 19. Zhang, S., Y. Park, J. Li, X. Lu, W. Zhang, and X. Zhang, “Negative refractive index in chiral metamaterials,” *Phys. Rev. Lett.*, Vol. 102, 023901, 2009.
 20. Jin, Y., J. He, and S. He, “Surface polaritons and slow propagation related to chiral media supporting backward waves,” *Phys. Letters A*, Vol. 351, 354–358, 2006.
 21. Dong, J. F., Z. J. Wang, L. L. Wang, and B. Liu. “Novel characteristics of guided modes in chiral negative refraction waveguides,” *Proceedings of International Symposium on Biophotonics, Nanophotonics and Metamaterials, Metamaterials 2006*, 517–520, Oct. 2006.
 22. Zhang, C. and T. J. Cui, “Chiral planar waveguide for guiding single-mode backward wave,” *Opt. Commun.*, Vol. 280, No. 2, 359–363, 2007.
 23. Cheng, Q., T. J. Cui, and C. Zhang, “Waves in planar waveguide containing chiral nihility metamaterial,” *Opt. Commun.*, Vol. 276, No. 2, 317–321, 2007.
 24. Naqvi, Q. A., “Planar slab of chiral nihility metamaterial backed by fractional dual/PEMC interface,” *Progress In Electromagnetics Research*, PIER 85, 381–391, 2008.